SAO-AXAF-DR-94-083
Data Type: 3
Rev "A"
February 1994

Advanced X-Ray Astrophysics Facility (AXAF)

Mission Support

NAS8-36123

Performance Reports:

AXAF VETA-I Mirror Ring Focus Measurements

Prepared in accordance with DRD# 784MA-002

Principal Investigator

Dr. H. D. Tananbaum

Prepared for:
George C. Marshall Space Flight Center
National Aeronautics and Space Administration
Marshall Space Flight Center, AL 35812

Submitted by:
Smithsonian Astrophysical Observatory
60 Garden Street
Cambridge, MA 02138

The Smithsonian Astrophysical Observatory
is a member of the
Harvard-Smithsonian Center for Astrophysics

SAO-AXAF-DR-94-083
Data Type: 3
Rev "A"
February 1994

Advanced X-Ray Astrophysics Facility (AXAF)

Mission Support

NAS8-36123

Performance Reports:

AXAF VETA-I Mirror Ring Focus Measurements

Prepared in accordance with DRD# 784MA-002

Principal Investigator

Dr. H. D. Tananbaum

Prepared for:
George C. Marshall Space Flight Center
National Aeronautics and Space Administration
Marshall Space Flight Center, AL 35812

Submitted by:
Smithsonian Astrophysical Observatory
60 Garden Street
Cambridge, MA 02138

The Smithsonian Astrophysical Observatory
is a member of the
Harvard-Smithsonian Center for Astrophysics

Smithsonian Institution
Astrophysical Observatory

Title: Performance Reports:
AXAF VETA-I Mirror Ring
Focus Measurements

Date: 1 Feb 1994

Document No.: SAO-AXAF-DR-94-083

DRD No.: 784MA-002

Prepared by: P. Zhao

Data Type: 3

Filename: (c:MA002.083)

Revision: "A"

APPROVAL SIGNATURES

Deputy F. Cocuzzo 3/29/94
Program Manager Date

Smithsonian Institution
Astrophysical Observatory

REVISION HISTORY

Title: Performance Reports:
AXAF VETA-I Mirror Ring
Focus Measurements

Date: 1 Feb 1994

Document No.: SAO-AXAF-DR-94-083

DRD No.: 784MA-002

Prepared by: P. Zhao

Data Type: 3

Filename: (c:MA002.083)

Revision: "A"

Revision Record

Revision	Date	DCO No.	Affected Pages
"A"	1 Feb 94	-------	Initial Release

AXAF VETA-I Mirror Ring Focus Measurements

Ping Zhao, Mark D. Freeman, Diab Jerius, and Yibo Shao

Harvard-Smithsonian Center for Astrophysics
60 Garden Street, Cambridge, MA 02138

ABSTRACT

The AXAF VETA-I mirror ring focus measurements were made with an HRI (microchannel plate) X-ray detector. The ring focus is a sharply focused ring formed by X-rays before they reach the VETA-I focal plane. It is caused by spherical aberrations due to the finite source distance and the despace in the VETA-I test. The ring focus test reveals some aspects of the test system distortions and the mirror surface figure which are difficult or impossible to detect at the focal plane. The test results show periodic modulations of the ring radius and width which could be caused by gravity, thermal, and/or epoxy shrinkage distortions. The strongest component of the modulation had a 12-fold symmetry, because these distortions were exerted on the mirror through 12 flexures of the VETA-I mount. Ring focus models were developed to simulate the ring image. The models were compared with the data to understand the test system distortions and the mirror glass imperfection. Further studies will be done to complete this work. The ring focus measurement is a very powerful test. We expect that a similar test for the finally assembled mirror of AXAF-I will be highly valuable.

1. INTRODUCTION

The Advanced X-ray Astrophysical Facility (AXAF), a high resolution telescope for X-ray astronomy, is the third of NASA's four Great Space Observatories [1]. AXAF-I (for imaging) is scheduled to be launched in 1998. The heart of the AXAF-I is the largest X-ray mirror assembly ever built – the High Resolution Mirror Assembly (HRMA). The HRMA consists of four pairs of nested Wolter Type I grazing incidence mirrors. These nearly cylindrical paraboloid-hyperboloid mirror pairs are made of Zerodur and coated with iridium. Mirror diameters range from 0.64 m to 1.22 m with a length of 838.2 mm for each cylinder. The mean grazing angles range from 27.1 arcmin for the inner pair to 51.2 arcmin for the outer pair. The focal length of the HRMA is 10 meters.

The Verification Engineering Test Article I (VETA-I) was the uncoated and uncut outermost pair of the HRMA. The two VETA-I mirrors are called P1 (paraboloid) and H1 (hyperboloid). A test of the mirror glass surface quality was successfully performed on VETA-I at the X-ray Calibration Facility (XRCF) of the Marshall Space Flight Center from September 1 to October 18, 1991. The test system used X-ray sources 528 meters from the VETA-I and two kinds of detectors to measure the focused X-rays. Because the P1 and H1 were not cut to the design length, they had to be spaced 109.03 mm farther apart than the design spacing during the test (this fact is called despace). The mirror is designed to focus incident X-rays from infinitely distant sources. For the ground test with a finite source distance and despace, there are two interesting focal planes where our measurements were made (see Figure 1). One is called the overall focal plane or the finite-distant focal plane (hereafter referred to as the focal plane), and is located farther away from the mirror than the designed focal length. This is the location of the waist of X-rays focused by the entire mirror. The other is called the ring-focus plane and is located in between the on-orbit focal plane and the finite-distant focal plane. In the ring-focus plane, X-rays form a sharply focused ring before reaching the focal plane . The ring focus is caused by spherical aberration in the VETA-I test. In the focal plane, we measured FWHM (this is the main goal of the VETA-I test), encircled energy and effective area. The results of these measurements were discussed in 16 papers published in the SPIE '92 proceedings [2]. There is also a paper [3] discussing the result of a ring focus measurement made over a small sample of the ring with a proportional counter. The present paper discusses the ring focus measurements with a microchannel plate, presents the results, and compares the results with models of the mechanical distortions of the mirror glass.

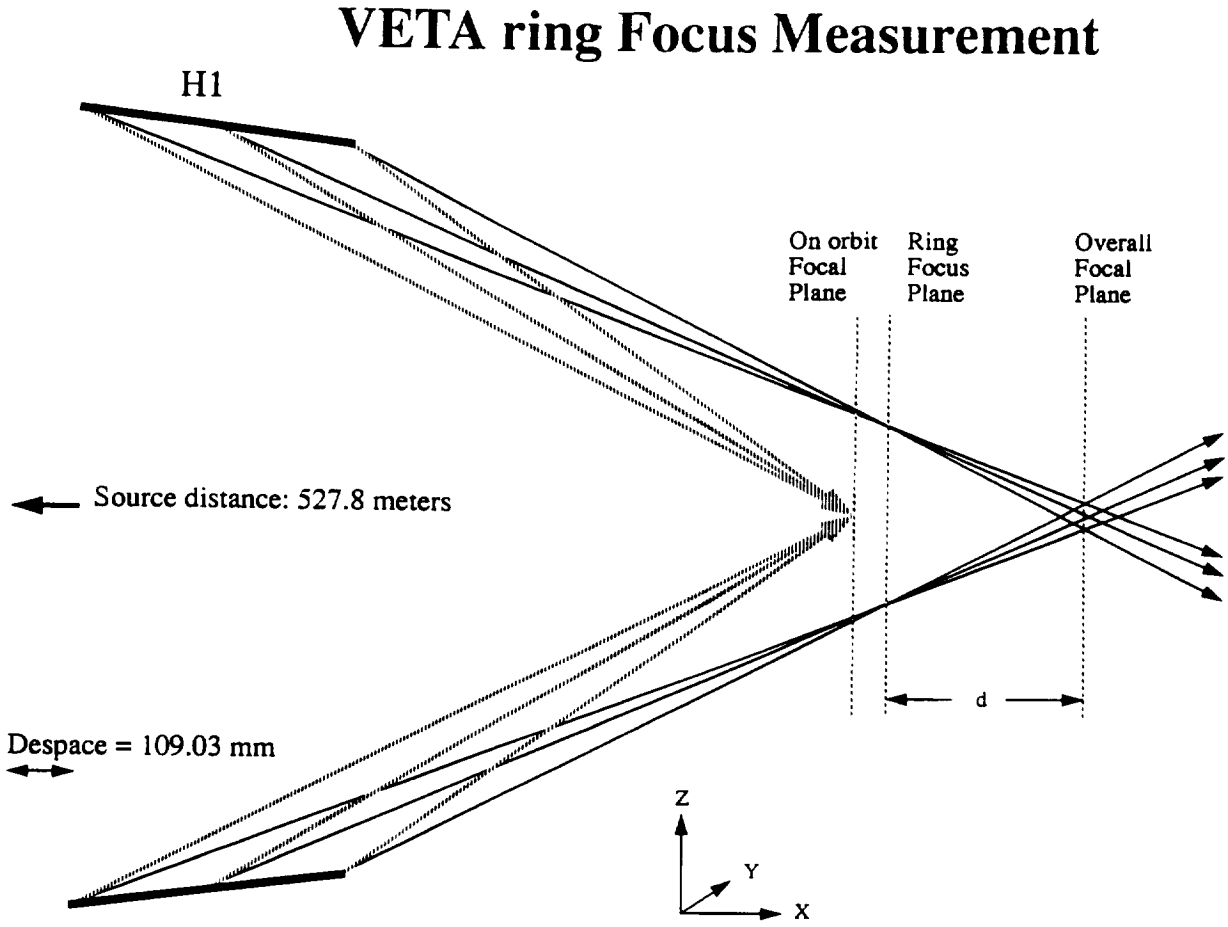

Figure 1: VETA-I ring focus measurement. The VETA-I mirror pair consists of a paraboloid (P1, not shown) and a hyperboloid (H1). Rays shown in the figure are reflected by the H1. The ring focus is caused by spherical aberrations due to finite source distance and despace in the VETA-I test.

2. RING FOCUS

The ring focus test for the AXAF mirrors was originally proposed by D. Korsch and D.E. Zissa [4, 5]. This test is applicable to an optical system that has a narrow annular aperture and also has spherical aberration, which is appropriate for VETA-I, where the spherical aberration was caused by finite source distance and despace. The ring focus test is complementary to the focal plane tests. It reveals some aspects of the test system distortion and the mirror surface figure which are difficult or impossible to detect in the focal plane. Our motivations to perform the ring focus test can be summarized as follows:

- The image at the focal plane is large due to the spherical aberration.
- Low frequency errors are collapsed together in the focal plane.
- The separation of mirror surface errors and the test system effects is easier at the ring focus plane.

For a perfect optical system, the ring is sharply focused but its width is not infinitesimal. The width

of the ring is a function of the spherical aberration of the system. It can be calculated accurately for a perfect optical system. If VETA-I was a perfect mirror and the test system was also perfect, the ring width solely due to the system spherical aberration, the finite source distance and the despace, should be 0.148 μm. However, in the real VETA-I system, the mirror surface errors and the test system properties cause the ring image to be distorted and blurred, and the ring width to be broadened. Factors that could cause the ring width broadenings are:

1. Theoretical test geometry (Square functions: 0.003 arcsec, 0.148 μm at the ideal ring focus plane; 0.5 arcsec, 26.5 μm at the actual ring focus measurement plane. See Section 3).
2. Source size ($\sim$ 0.12 arcsec, 6 μm FWHM).
3. Detector resolution ($\sim$ 0.5 arcsec, 25 μm FWHM).
4. Mounting system induced distortions: Gravity, Thermal, epoxy shrinkage.
5. Mirror glass surface imperfections.

The ring width broadenings due to the first three factors can be calculated accurately based on the experimental data we obtained before the VETA-I test. The effects of the fourth factor were not well known at the time of the test. They have to be extrapolated by comparing the test data with the ring focus models which we will discuss in section 5. The fifth factor – mirror surface imperfections – is the one we want to measure. Our goal is to separate the system errors (the first 4 factors) and the mirror surface error (fifth factor) from the test data.

3. MEASUREMENTS

The ring focus measurements were carried out after the VETA-I focal plane measurements. There was no precise measurement (to submillimeter level) of the distance between the VETA-I mirrors and the focal planes. So the axial coordinate difference between the ring and finite-distant foci was used for measurements and data analysis. Defining the optical axis as the X-axis (pointing from mirrors to the focus) and if the on-orbit focus is at X = 0, the X offsets of the ring focus plane and the focal planes are 39.70 mm and 218.42 mm, respectively, based on a ray-trace calculation for a perfect VETA-I system. Thus the distance between the two focal planes is 178.72 mm for a perfect system.

The C-K line was the only X-ray source used for the ring focus measurements. The measurements were made with two kinds of detectors: 1) a gas proportional counter with vertical and horizontal slits (9.5 μm $\times$ 290 μm); and 2) a microchannel plate detector (HRI: High Resolution Imager) with a resolution of 25 μm (FWHM). Because of mirror and test system distortions, the actual ring focus plane (i.e. the plane containing the narrowest ring width) is not located 178.72 mm from the focal plane. To search for the actual ring focus plane, the proportional counter was placed at six locations on the X-axis to measure the ring width. The measurements were made as the counter and its horizontal (vertical) slit aperture scanned across the top and bottom (left and right) portions of the ring [3]. The results show that the actual radial profiles of the ring had triple peaked structures varying with the azimuthal angle. The minimum ring width RMS for top and bottom (left and right) portions of the ring were formed at different X positions. Therefore, there was no single plane at constant X that could be referred to as the actual ring focus plane. A plane was chosen with a compromise X position – 215.1 mm from the focal plane – where the ring widths for both top and bottom were relatively narrow. HRI images were then taken in this plane. Because the ring size (25.5 mm diameter) is larger than the HRI, four images were taken for top, bottom, left and right quadrants of the ring. Each image had an exposure time of 30 minutes. While the proportional counter with slits could only measure (with slightly higher resolution) the radial profiles at four locations, the HRI measurements can reveal the radial profile at any azimuthal angle around the ring.

However, the X position of the ring images taken – 215.1 mm – is rather far from the ideal ring focus plane. Based on lessons learned from our data analysis, we should perform the measurements at the ideal ring focus plane in the future. (If time allows, we can do it in both ideal and actual ring focus planes.) The reasons are the following: 1) Because the depth of focus of the ring is relatively large, it is difficult to find the actual ring focus plane accurately and efficiently, and due to the system tilt, there may not be a single

actual ring focus plane; and 2) Detections of the test system effects are easier for images in the ideal ring focus plane.

4. DATA ANALYSIS

The four images taken with the HRI were digitized to readout pixels of 6.45 μm × 6.45 μm. Each image collected about 0.3 million photons. Before the data analysis, the HRI scale was carefully measured and evaluated. One of the processes is called degap. The HRI readout is a crossed grid charge detector, which consists of two orthogonal planes of wires electrically separated from each other. These two wire plates are located behind the microchannel plate stack to collect the charge. The electron charge cloud has a core/halo type of structure and spreads over several wires. A fine position algorithm was developed to determine the centroid of the charge cloud to a small fraction of the wire spacing. An artifact due to this algorithm is 16 vertical and 16 horizontal gaps left in the raw images [6]. The degap process restores the image so that each pixel appears at its actual location. Figures 2 and 3 show a ring image before and after the degap process. In order to capture the entire ring with the HRI, this image was taken at a position in between the ring focus plane and the focal plane, where the ring is smaller. Four large gaps at ± 45° and ± 135° on the ring were due to the VETA-I supporting struts. Figure 4 shows the four images of the ring focus measurements after the degap.

Based on these four images and the HRI motor position log, a common ring center was located on each of the quadrant images. The ring images were then divided into annuli and pie sectors with respect to this common center, using the IRAF/PROS (Image Reduction and Analysis Facility / Post-Reduction Off-line Software) software. In the vicinity of the ring, each annulus was chosen to be one pixel (6.45 μm) wide. Each sector was 2° which gives adequate statistical errors and azimuthal resolution. Photon counts in each cell of the annulus-sector grid were tabulated. Radial profiles near the ring for each azimuthal angle were then plotted, as shown in Figures 5 and 6. For some parts of the ring, the width and the radius stay the same for different azimuthal angles (Figure 5); while for other parts, they change drastically (Figure 6).

The ring width RMS and FWHM, and mean radius were calculated for each radial profile. There were a large number of scattered photons in each image. Because a photon far away from the ring can carry large statistical weight, the above calculations are meaningless without clipping. Therefore, a window of 250 μm was set around the ring in order to perform the calculations. Inside this window, focused photons were strongly dominant over the scattered photons. All the photons outside this window, where scattered photons were dominant, were ignored. Thus the photon scattering does not affect the ring focus data analysis and is not considered in the ring focus models discussed later. We did not intend to use the ring focus data to measure the scattering from the mirror surface, which was done by using the focal plane data.

In Figure 7, the top panel is a plot of the ring width RMS vs. the azimuthal angle. (We chose RMS to represent the ring width because it carries a better statistical value than FWHM.) When looking towards the +X direction, 0° is on the bottom of the ring; 90° is on the left; 180° is on the top; and -90° is on the right. The 4 gaps due to the supporting struts were filled with a spline fitting function. A modulation with a 30° period is clearly shown in this figure. The bottom panel of Figure 7 is the Fourier transformation of the top panel, plotted as the modulation power vs. the frequency in one circumference. The modulation has dominant frequencies of 2 (180° period), 12 (30° period) and its higher harmonics. Figure 8 shows the ring mean radius plot and its Fourier transformation. It also has a 12-fold symmetry, i.e. a modulation frequency of 12.

5. MODELS

The ring focus models are images, computer generated by ray-tracing to simulate the X-rays passing through the VETA-I mirror and the test system. The VETA-I models used in the ray-trace were built, as a joint effort of SAO and Kodak, according to our best knowledge of the VETA-I test system. At the present time, the mirror surface errors (such as circumferential slope error, axial slope error, $\Delta\Delta R$, sag, etc.) are

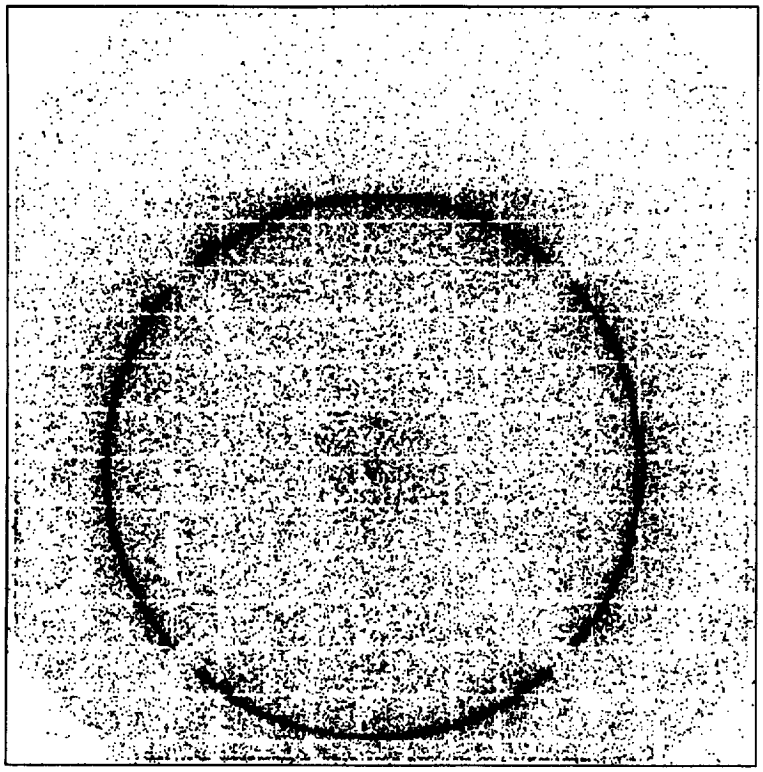

Figure 2: VETA HRI Image before the degap.

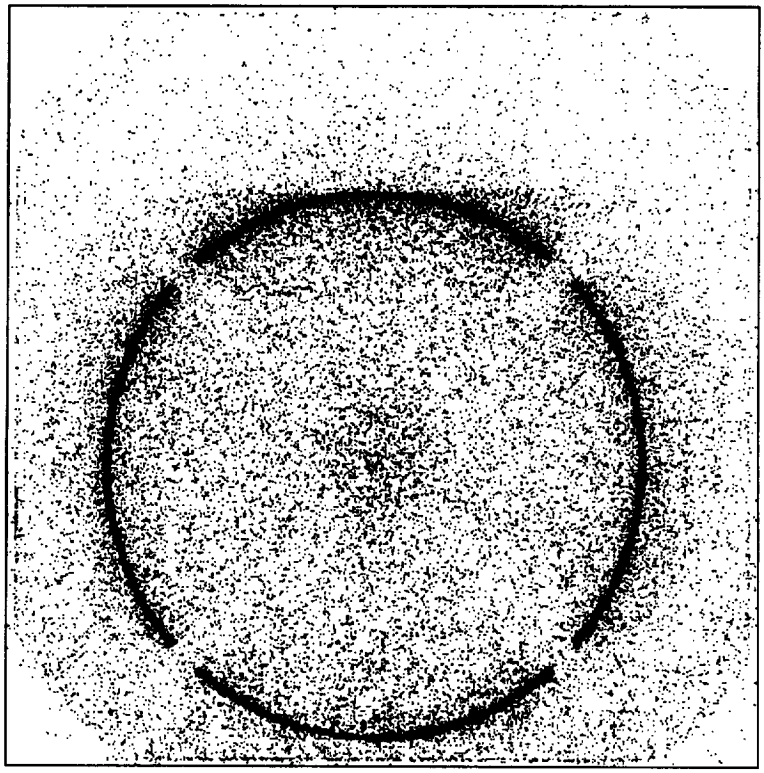

Figure 3: VETA HRI Image after the degap.

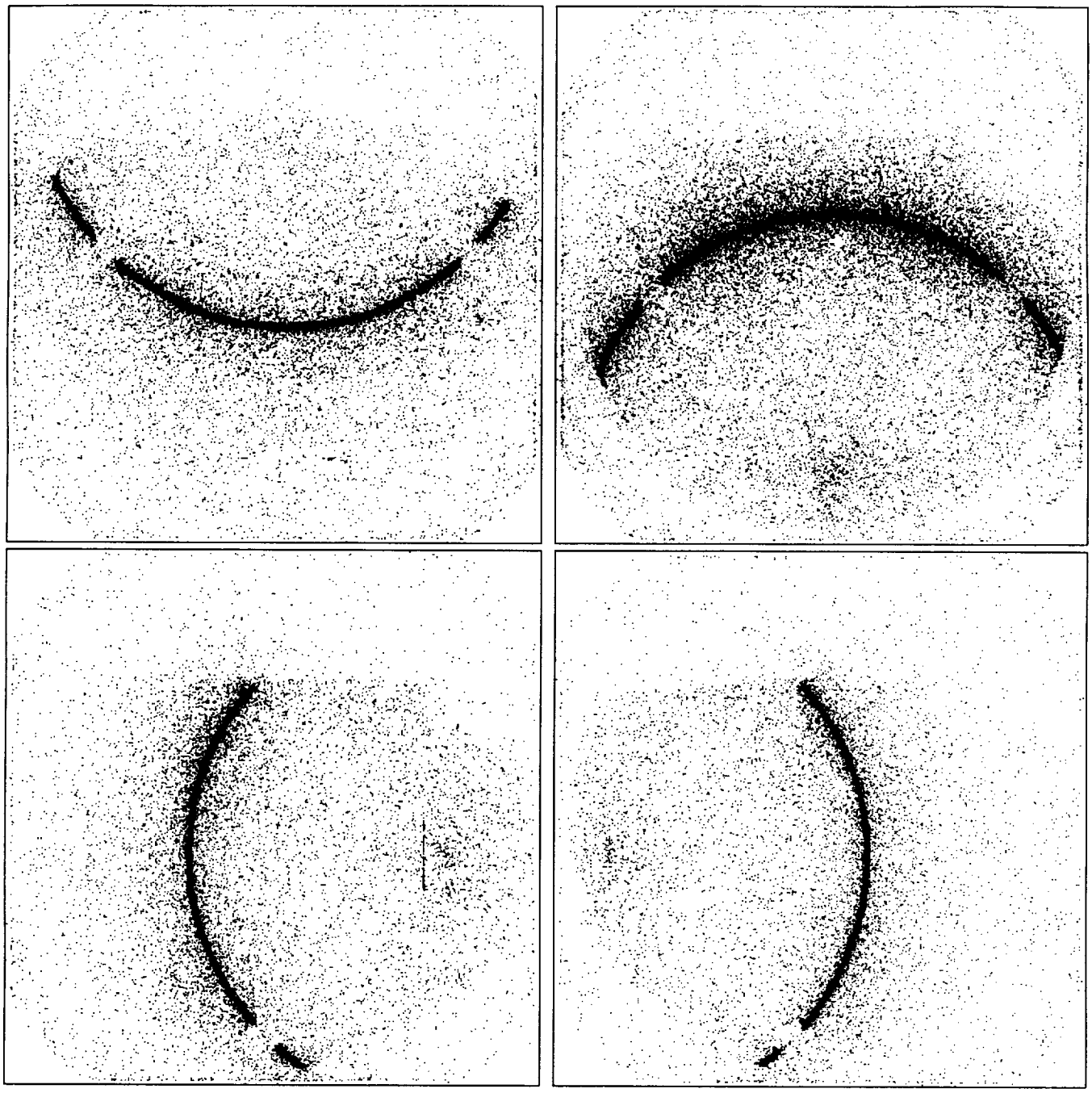

Figure 4: Four HRI images of the VETA ring focus.

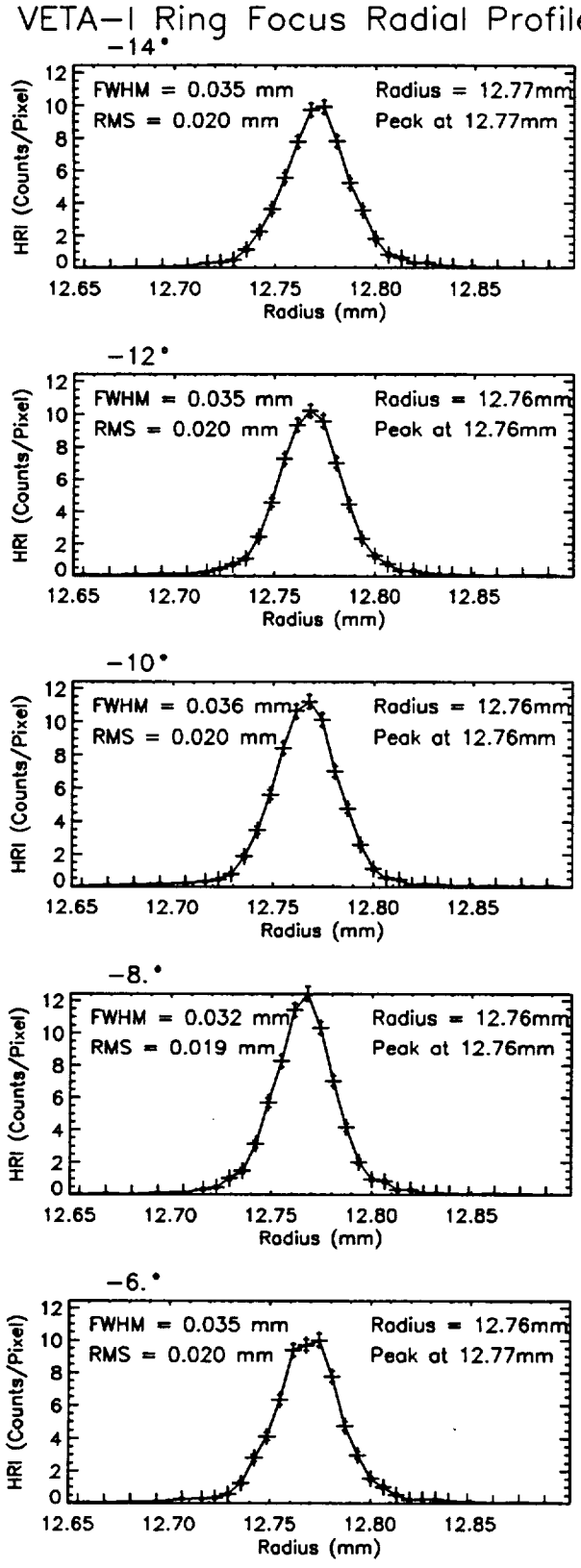

Figure 5: VETA ring focus radial profile. No significant change in the ring radius and width.

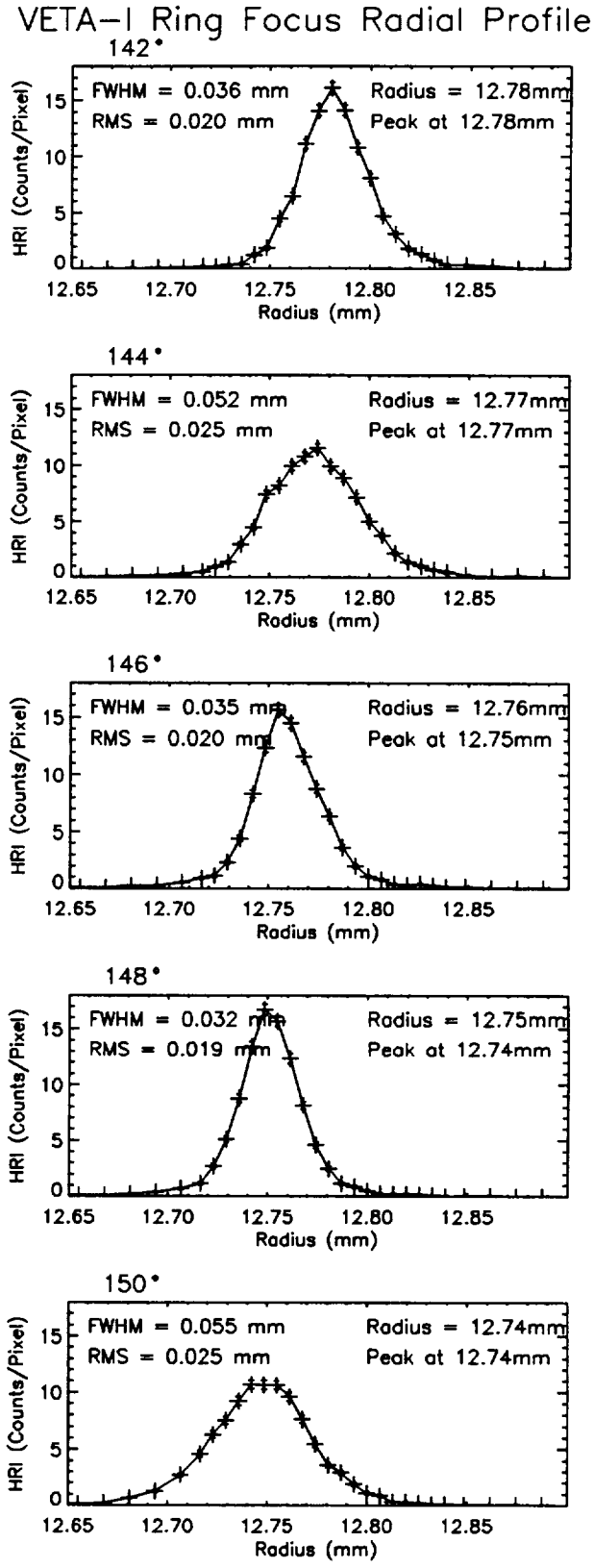

Figure 6: VETA ring focus radial profile. The ring radius and width change with azimuthal angle.

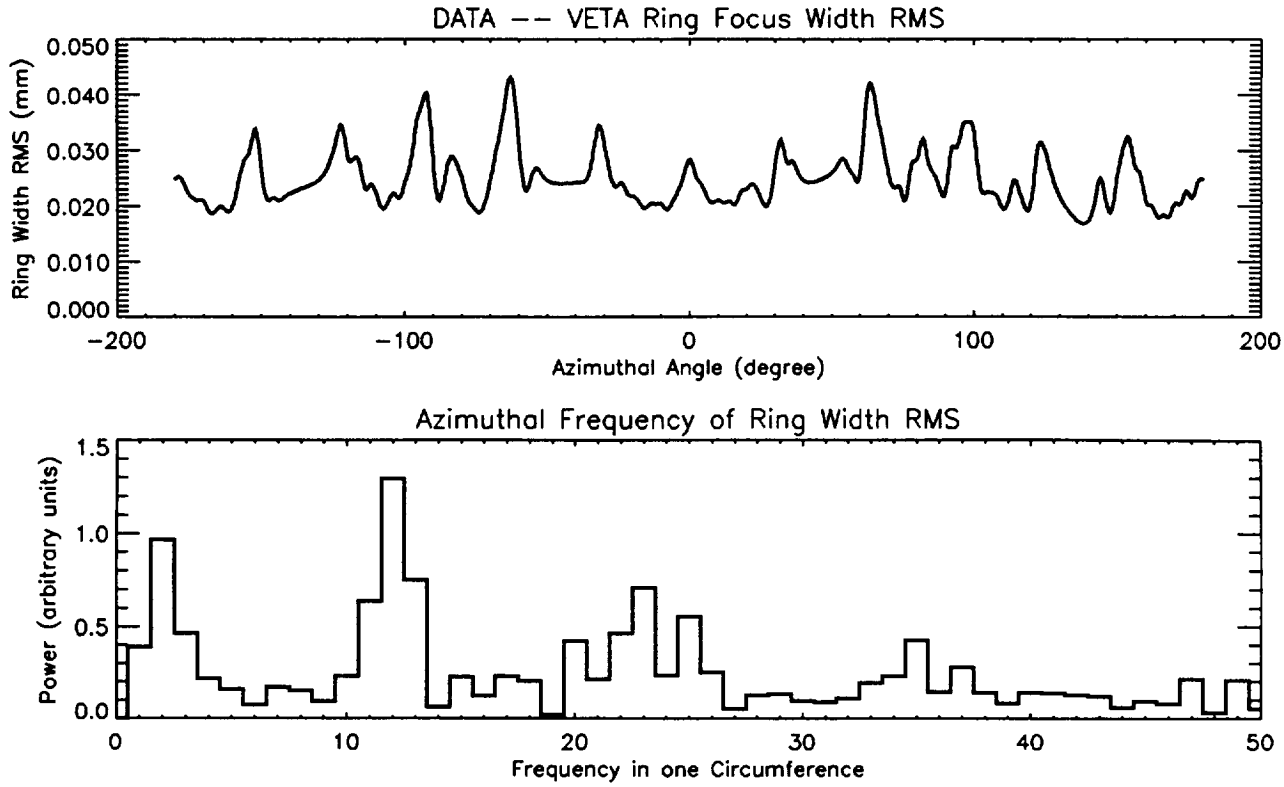

Figure 7: VETA data – ring focus width RMS.

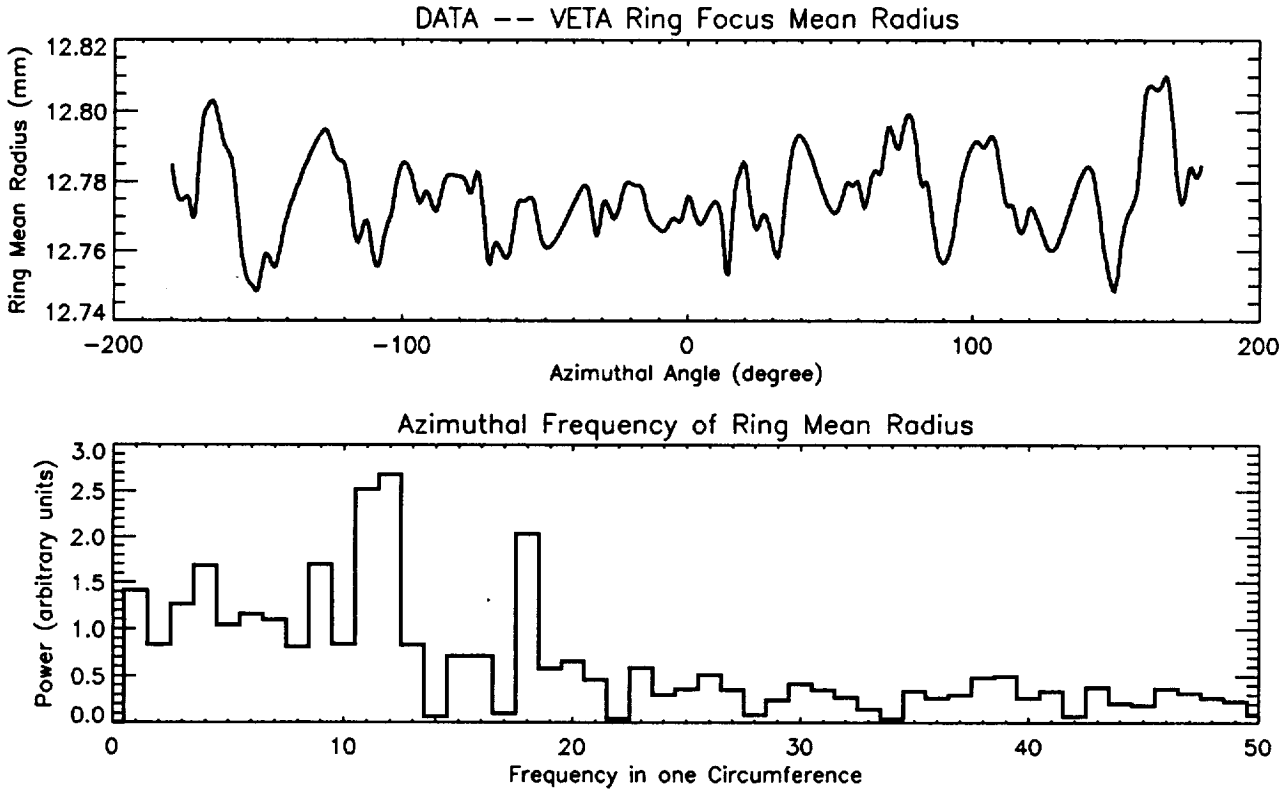

Figure 8: VETA data – ring focus mean radius.

not built into the VETA-I model. Our current study involves: 1) Building the VETA-I model solely based on the test system induced distortions; 2) Comparing the model with the ring focus data to understand the test system; 3) Extracting the mirror surface errors and comparing them with metrology data obtained from the optical test. After this study we will build complete VETA-I models including both system and mirror surface errors.

As mentioned earlier, we understood the test geometry (the source distance, mirror position and tilt, detector positions, etc.) very well. The VETA-I mounting system is the major concern in building the VETA-I model. Each one of the VETA-I mirrors (P1 and H1) was held by 12 flexures in the middle of the cylinder (see Figure 9 [7]). The flexures were made of titanium and located at the same positions as the 12 hours on a clock. Attached to the middle of each flexure was an invar pad, which was epoxied to the outside of the mirror. The 12 flexures were attached to an aluminum ring of the VETA-I mount. There were three mounting system induced distortions:

1. **Gravity & compensation:** At the beginning of the VETA-I test, it was found from measurements in the focal plane that the mirror was ovalized under the earth's gravitation, i.e. the mirror diameter in the horizontal direction is slightly larger than that in the vertical direction. This distortion was promptly corrected by applying squeezing forces on the two sides of the mirror. This was called the gravity compensation for the global effect. But the gravity also had local effects which were not compensated. As illustrated in Figure 10 [7], because the mirror was hung at 12 rather small areas (1 inch $\times$ 1 inch), the gravity caused local distortions at those 12 locations. The distortions along the sides of the mirror were more severe than at the top or bottom. These local distortions would cause a shifted 12-fold symmetry (i.e. near 11 or 13 fold) and possibly a 2-fold symmetry due to the fact that the side distortions were different from the top and bottom. An over or under squeezed mirror would also have a 2-fold symmetry.

2. **Thermal effects:** The 12 flexures were attached to an aluminum ring which has a high thermal expansion coefficient. In contrast, the Zerodur mirror is well known for its extremely low thermal expansion. If the test temperature was different from the temperature when the mirror was mounted, the aluminum ring would pull or push the mirror through the flexures and invar pads at the 12 mounting points (see Figure 11). A uniform thermal effect should cause a symmetric distortion on the mirror and therefore a 12-fold symmetry in the ring focus image. A non-uniform thermal effect could cause an asymmetric distortion on the mirror.

3. **Epoxy shrinkage:** The shrinkage of epoxy between the invar pads and the mirror could cause local distortions in the mirror plane as well as in the direction normal to this plane. Assuming the amount of the epoxy is about the same under each pad, this distortion is also symmetric and hence produces a 12-fold symmetry in the ring focus image.

Table 1 lists all the distortions for a complete VETA-I ring focus model. Our current model includes all of them except the mirror surface errors which we aim to obtain by comparing the model with the ring focus data. Parameters used for source distance, source size, despace and detector resolution were accurately measured. Errors due to alignment between P1, H1 and optical axis were estimated according to the focal plane data. The mount induced distortions were provided by Kodak. The gravity and compensation distortion was calculated based on the actual squeezing force applied. The thermal effect was calculated based on the test temperature record measured around the mirror during the test. The temperatures at different locations around the mirror varied between 70.0 °F (the nominal temperature) and 70.2 °F. The distortion due to such a small temperature variation is actually negligible, so there is no significant thermal induced 12-fold symmetry in the model. Compared to the ring focus data, the epoxy shrinkage distortion appears to be larger than the original prediction. Our current model contains the epoxy shrinkage distortion with a factor 3 greater than the predicted value. The ring focus model was then made with 20 million rays tracing through the VETA-I model. Figures 13 and 14 show the ring width RMS and ring radius as well as their Fourier transforms based on our current VETA-I ring focus model.

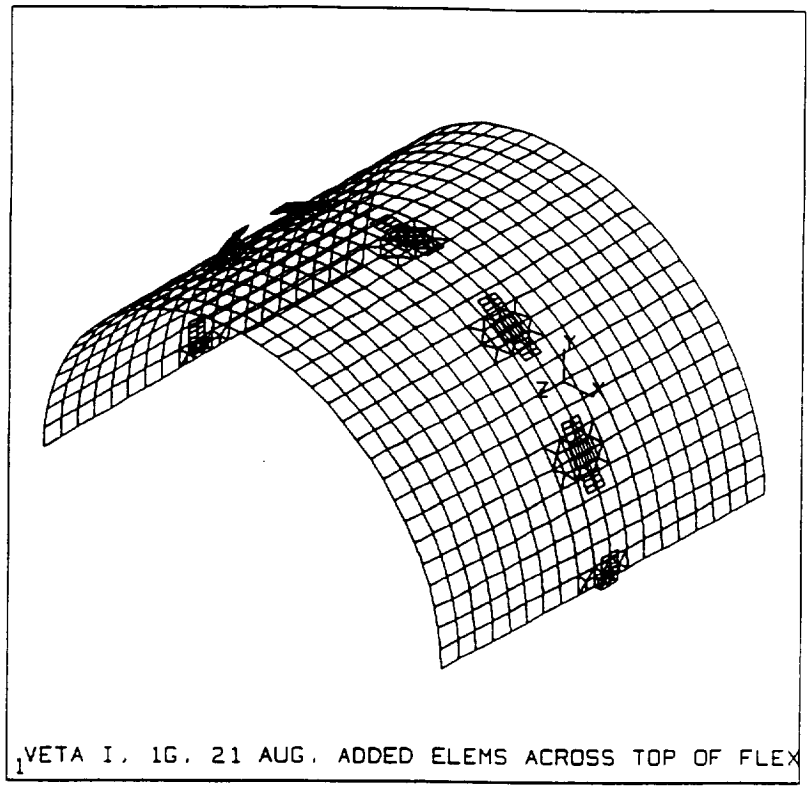

Figure 9: Each VETA-I mirror was held by 12 flexures in the middle of the cylinder.

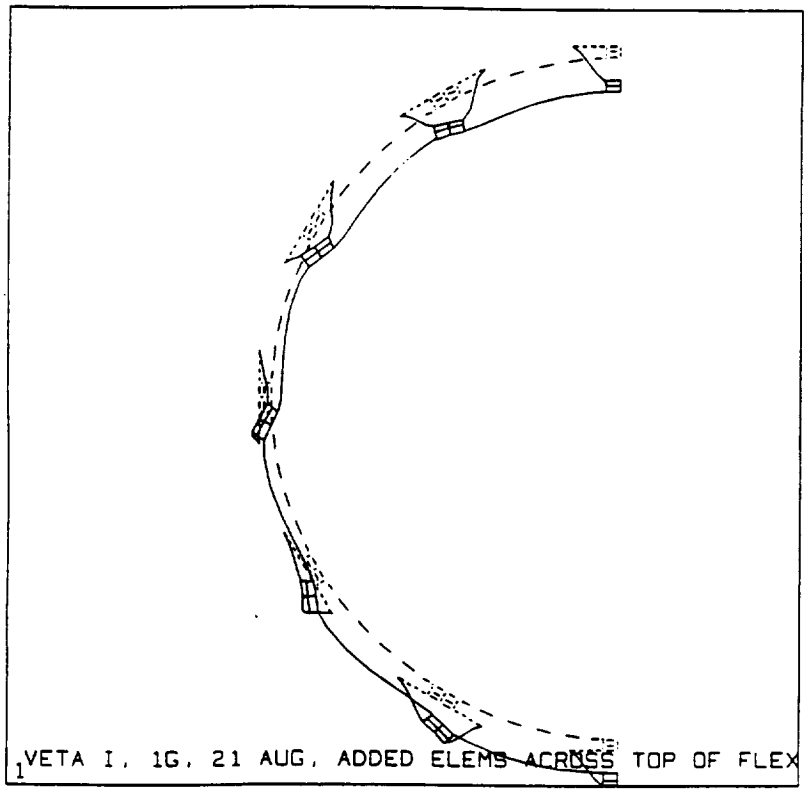

Figure 10: Gravity caused mirror local distortions near 12 flexures. Distortions along the sides of the mirror were more severe than at the top or bottom.

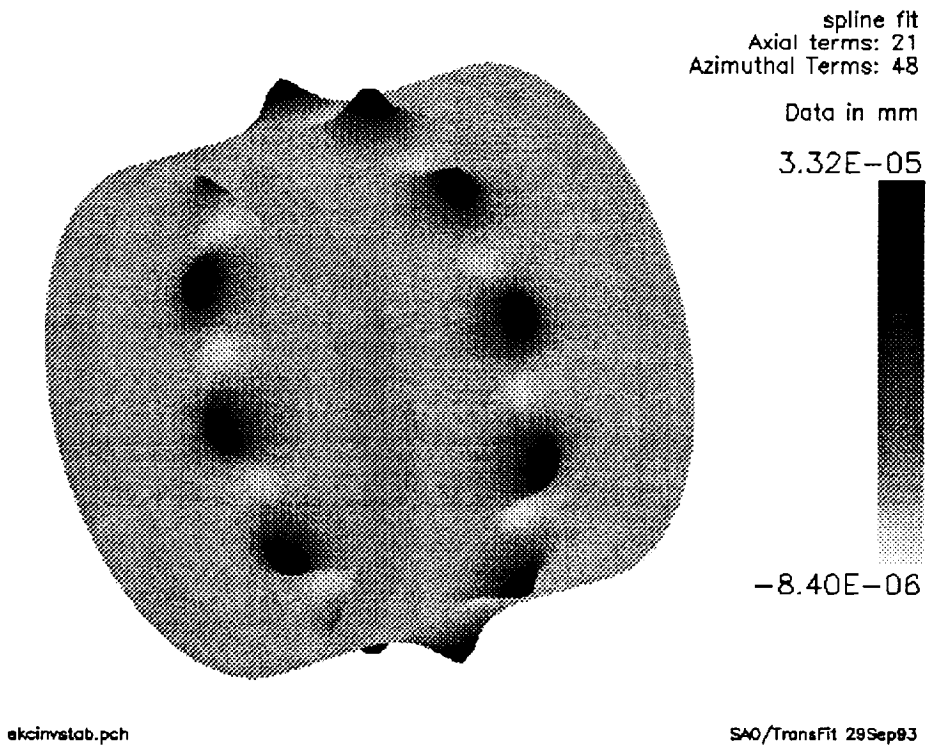

Figure 11: The mirror 12-fold distortion model due to the uniform thermal effect and/or epoxy shrinkage.

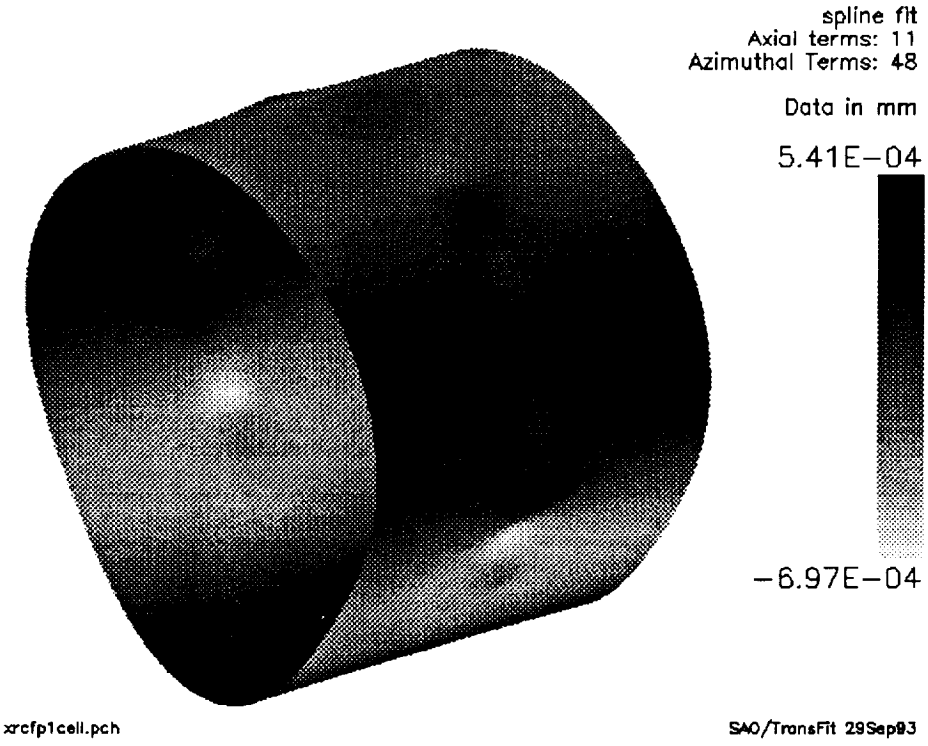

Figure 12: The mirror 1-g deformation model with the gravity compensation.

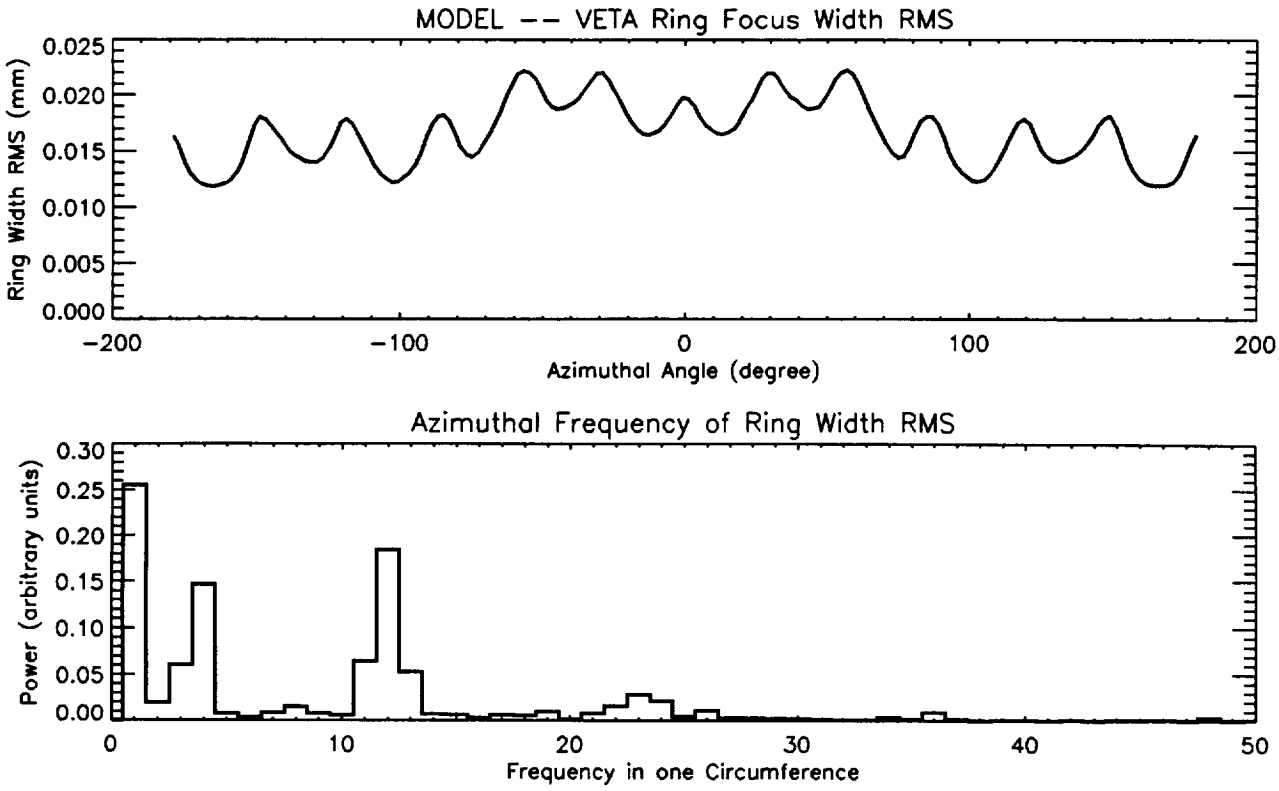

Figure 13: VETA model – ring focus width RMS.

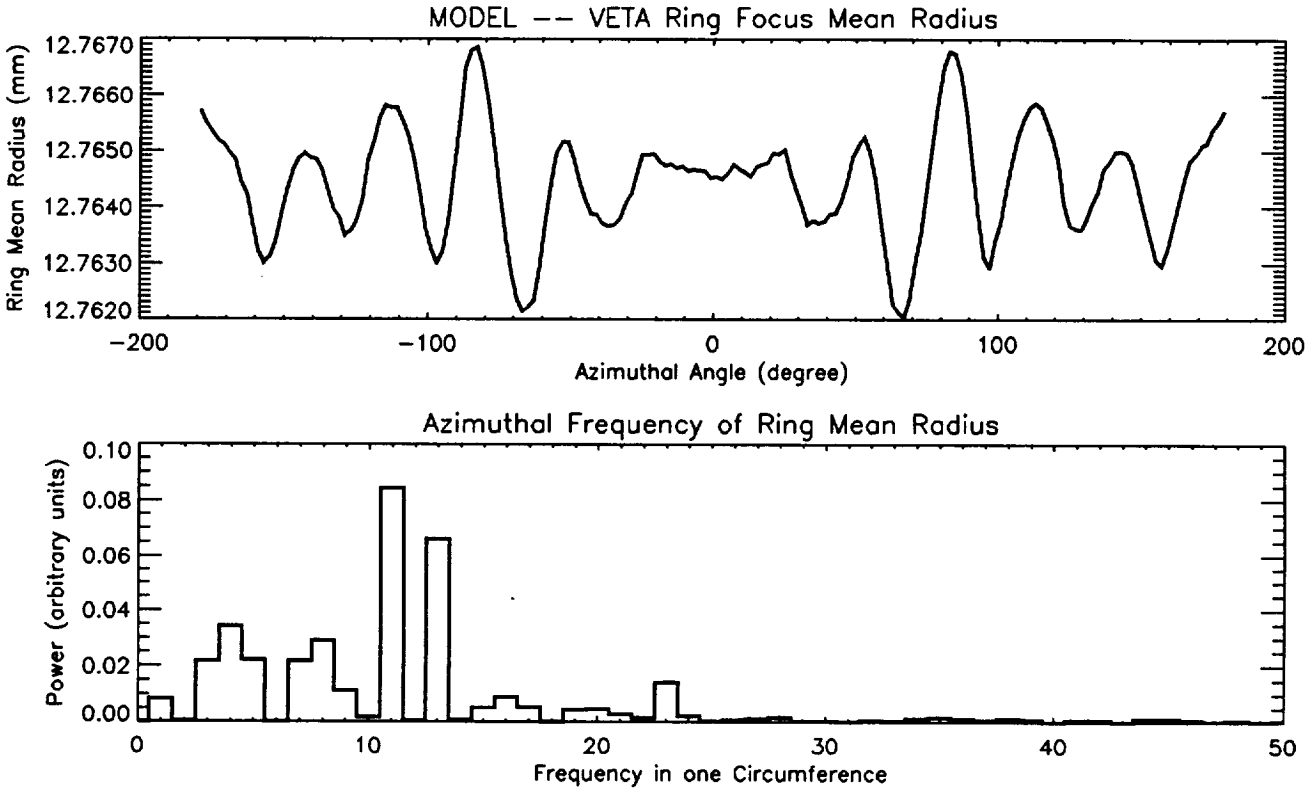

Figure 14: VETA model – ring focus mean radius.

Table 1. VETA Ring Focus Model

Complete Model	Current Model	Parameters for Models
Test geometry:		
Source distance	Yes	Measured
Source size	Yes	Measured
Despace	Yes	Measured
Detector resolution	Yes	Measured
Alignment errors	Yes	Estimated
Mount induced distortions:		
Gravity & compensation	Yes	Calculated
Thermal effects	Yes	Calculated
Epoxy shrinkage	Yes	Estimated
Mirror surface errors (To be measured)	No	From optical test

6. COMPARING DATA WITH MODEL

Having reduced the data and established a model, comparing the two brings us to the central part of this work. Readers can do this themselves by simply comparing Figures 7 and 8 to Figures 13 and 14. Table 2 is a list of the comparisons. We now discuss them one by one:

Table 2. Comparisons of VETA Ring Focus Data With Model

Symmetry	Data	Model	Comparison & Discussion
Ring Radius			
12 fold	Strong	None	Data show symmetric distortions.
11,13 fold	Weak	Strong	local 1-g effect dominates the model.
Ring Width			
1 fold	Weak	Strong	Model has wider ring width at the bottom than the top.
2 fold	Strong	Weak	Data show strong local 1-g effect on both sides of mirror.
4 fold	Weak	Strong	Model has stronger 4 fold symmetry than data.
12 fold	Strong	Strong	Data and model both show symmetric distortions.
11,13 fold	Yes	Yes	Data and model both show local 1-g effect.
Base width	20μm	12μm	Mirror glass imperfection caused broadening $= \sqrt{20^2 - 12^2} = 16\mu$m.

Ring Radius:

- **12-fold symmetry:** The data show strong 12-fold symmetry with large variations on the ring radius ($\pm$ 30 μm), which is likely due to the temperature change, epoxy shrinkage in the normal direction of the surface and/or other mechanical effects causing the 12 invar pads to exert force normal to the mirror surface. This symmetric distortion is absent in the model.

- **11,13-fold symmetries:** The model has dominant 11 and 13-fold symmetries. In the data, these are weaker than the 12-fold symmetry. The 11 and 13-fold symmetries are due to the local gravity effect acting on those 12 supporting points outside the mirror. In other words, it is caused by the beating between $cos(\theta)$ (gravity) and $cos(12\theta)$ (flexures):

$$cos(\theta)[cos(12\theta) + cos(24\theta) + \cdots] = \tfrac{1}{2}[cos(11\theta) + cos(13\theta) + cos(23\theta) + cos(25\theta) + \cdots]$$

  This beating effect is clearly seen in Figure 14. However, the amplitude of the modulation ($\pm$ 2.5 μm) in the model is much smaller than the 12-fold modulation in the data ($\pm$ 30 μm). This is an indication that the model underestimated the 12-fold symmetry and/or overestimated the local gravity effect which caused available 12-fold modulation completely shifted to 11 and 13-fold.

Ring Width

- **1-fold symmetry:** The model has a dominant 1-fold symmetry. This means that the modulation with the lowest frequency (360° period) has the largest amplitude. This is seen in the top panel of Figure 13: The base-width RMS near 0° (17 μm) is 40% higher than that near 180° (12μm). It is not clear at the moment why the model has a wider ring width at the bottom than at the top. It is possibly due to an inaccurate gravity model.

- **2-fold symmetry:** For ring width RMS, the 2-fold symmetry shown in its Fourier transform is strong in the data and very weak in the model. This effect is clearly seen in the top panel in Figure 7, where the ring width modulation amplitudes along the sides ($\pm$ 90°) of the mirror are more than twice as large as those near the top or the bottom (0° or 180°). In the model, there is no obvious change in the modulation amplitude. This indicates that the data show exactly the local gravity effect described in section 5. Even though the current model also shows the local gravity effect (11 and 13-fold symmetries in radius and width), it does not give an accurate account of the modulation amplitude.

- **4-fold symmetry:** The model shows a strong 4-fold symmetry, which is very weak in the data. This is another indication that the current 1-g model may inaccurately estimate the global gravity effect. Figure 12 is a 3-D surface plot of the P1 mirror according to the Kodak 1-g model. The plot indicates an overestimation of the gravity effect at $\pm$ 45° and $\pm$ 135°.

- **12-fold symmetry:** The data and model both show strong 12-fold symmetries, which could be caused by thermal and/or epoxy shrinkage distortions; however, there is a big difference (see Figures 7 and 13). The modulation in the data has sharper and higher peaks (20 – 43 μm); the modulation in the model has broader and lower peaks (12 – 22 μm). This means that the data show distortions localized near the invar pads and normal to the mirror surface, which agrees with the discussion given in the ring radius 12-fold symmetry – the 12 invar pads exerted forces normal to the mirror surface. The model has distortions extended to larger areas and distortions in the plane of the mirror surface, which are mainly caused by the epoxy shrinkage effect.

- **11,13-fold symmetry:** The data and the model both show 11 and 13 fold symmetries weaker than the 12-fold. Thus they both have the local gravity effects, which agree with what we observed in the ring radius.

- **Base Width:** The baseline (i.e. the narrowest part) of the ring width RMS is 20 μm for the data and 12 (top) – 17 (bottom) μm for the current model. This leaves a 10 – 16 μm ring width broadening due to the mirror glass surface imperfection. However, our current model is not complete, and we expect that the baseline will be higher after we improve the model. Therefore the ring width broadening due to the mirror surface error is expected to be less.

Our current model agrees with the data to a certain degree. There are some aspects in which the model does not give an accurate description of the actual VETA-I. We understand some of the inaccuracies and effects needed for improving the model. The gravity models used, both local and global, seem to be inaccurate and will be replaced. The current epoxy shrinkage model also needs improvement. However, there are aspects of the current model yet to be understood. For example, why is the ring radius modulation

amplitude larger at the sides of the mirror than that at the top or bottom, while the amplitude stays the same for the ring width?

We plan to further study the VETA-I ring focus results and theory to complete the model so that it can better match the data. We will then derive the mirror surface errors from the ring focus data by removing the distortions described by the model, and compare this error with the metrology data obtained from the optical tests of the P1 and H1 glass pieces subsequent to the VETA-I test.

7. SUMMARY

The ring focus measurement is potentially a very powerful test, which allows diagnosis of features not evident in the focal plane. High quality ring focus test data reveal large scale deformations of the mirror, induced by the test system distortions and the mirror surface errors, as a function of the azimuthal angle. We have carried out tests for the VETA-I mirror at the XRCF. The data was taken with HRI – a microchannel plate. The VETA-I ring focus models were generated by a ray-trace based on our best knowledge of the VETA-I test system. The model was compared with the data. It agrees with the data to a certain degree. We will continue this study to achieve a full understanding of the VETA-I mirror and its test system. During the study, we gained valuable experience in planning the ring focus test and building the VETA-I models. We expect that a ring focus test for the flight mirror of AXAF-I – HRMA – will be highly valuable.

8. HRMA RING FOCUS MEASUREMENTS

We have calculated the HRMA ring focus test geometry and designed the HRMA X-ray Detectors Assembly (HXDA) with the capability of moving the detectors between the focal plane and the ring focus plane accurately. Table 3 lists the HRMA ring focus geometry calculated for a perfect HRMA. Here the only cause of the ring focus is the finite source distance – a value of 528.74 meters between the X-ray source and the HRMA entrance plane was used for the current calculation. There will be four rings due to the four mirror shells of the HRMA. Because the mirrors will be cut to the design length and despace will be removed, the ring focus plane will be much closer to the focal plane than the VETA-I case. Also the sizes of the rings are much smaller. So we should be able to capture the entire ring image with a single exposure of HSI (High Speed Imager, a microchannel plane detector for the HRMA calibration which has 18 mm diameter and 16 μm FWHM resolution.) The HRMA ring focus measurements should be performed in a plane 65.1 mm from the focal plane towards the mirror.

Table 3. HRMA Ring Focus Geometry

Mirror Pair	Focal Plane X-offset	Ring Focus X-offset	Ring Focus to Focal Plane	Ring Radius	Ring Width
1	193.899 mm	129.246 mm	64.653 mm	3.83244 mm	1.2112 micron
3	194.011 mm	128.993 mm	65.018 mm	3.10215 mm	1.0267 micron
4	194.068 mm	128.887 mm	65.181 mm	2.74471 mm	0.9268 micron
6	194.129 mm	128.722 mm	65.407 mm	2.04695 mm	0.7115 micron

Mirror pair 1 is the outermost pair; 6 is the innermost pair.
The optical axis is defined as the X-axis. The on orbit focal plane is defined to be at X = 0.
Focal Plane X-offset: the X coordinate of the finite-distant focal plane.
Ring Focus X-offset: the X coordinate of the ring focus plane.
Ring Focus to Focal Plane: distance between the ring focus plane and the finite-distant focal plane.

9. ACKNOWLEDGMENT

We would like to thank members of the VETA-I calibration team (scientists, engineers, programmers, and people from SAO, MSFC, TRW and Kodak) for their contributions to this work. We especially appreciate the critical comments from Harvey Tananbaum, Leon Van Speybroeck, Daniel Schwartz, William Podgorski, Lester Cohen, John Hughes and Terrance Gaetz.

This work was partially supported under NASA Contract # NAS8-36123.

References

[1] M. C. Weisskopf, "The Advanced Astrophysics Facility: An Overview," *Astrophysical Letters & Communications,* Vol. 26, pp. 1-6, 1987.

[2] Editors: R. B. Hoover and A. B. C. Walker, Jr., "Multilayer and Grazing Incidence X-ray/EUV Optics for Astronomy and Projection Lithography", *SPIE Proceeding* Vol. 1742, pp. 1-202, San Diego, 1992.

[3] D. E. Zissa, "Comparison of Ring-focus Image Profile with Predictions for the AXAF VETA-I Test", *SPIE Proceeding* Vol. 1742, 91, San Diego, 1992.

[4] D. B. Griner, D. E. Zissa, and D. Korsch, "Test Method for Telescope Using a Point Source at a Finite Distance", MSFC Center Director's Discretionary Fund Final Report, Project No. H20, NASA Technical Memorandum TM-86523, September 1985.

[5] D. E. Zissa and D. Korsch, "Experimental Evaluation of the Ring Focus Test for X-ray Telescope Using AXAF's Technology Mirror Assembly", MSFC Center Director's Discretionary Fund Final Report, Project No. H20, NASA Technical Memorandum TM-86570, October 1986.

[6] J. H. Chappell and S. S. Murray, "Position Modeling for the AXAF High Resolution Camera (HRC)", *SPIE Proceeding* Vol. 1159, 460, San Diego, 1989.

[7] L. M. Cohen, "Preliminary Structural/Performance Analysis of Eastman Kodak VETA-I", SAO Memorandum to W. A. Podgorski, October 30, 1989.